Kinematic Modelling of Hybrid Parallel-Serial Five-Axis Machine Tool

Milan Milutinović
Lecturer
Tehnikum Taurunum - High Engineering
School of Vocational Studies

Nikola Slavković
Teaching Assistant
University of Belgrade
Faculty of Mechanical Engineering

Dragan Milutinović
Full Professor
University of Belgrade
Faculty of Mechanical Engineering

Compared with serial structured machine tools and robots, parallel kinematic machine tools and robots have many advantages. Many different topologies of parallel mechanisms with 3-6 DOF have been used. Considering that some limitations are indeed due to the use of parallel mechanisms, it is appealing to investigate architectures based on hybrid arrangements where serial and parallel concepts are combined. This paper is aimed at presenting a study on the kinematic modelling of the Tricept based five-axis vertical machine tool. Since the machine comprises 3-DOF parallel structure and 2-DOF serial wris,t direct and inverse kinematics also comprise serial and parallel part. Inverse kinematics is solved analytically while direct kinematics consists of an analytical and numerical part. Based on machine inverse kinematics, the workspace has been analysed in order to select machine prototype design parameters.

Keywords: hybrid mechanism, kinematic modelling, machine tool.

1. INTRODUCTION

Compared with serial structured machine tools and robots, parallel kinematic machine tools and robots have many advantages. Basic knowledge about diverse aspects of parallel kinematic machines has already been published. Many different topologies of parallel mechanisms with 3-6 DOF has been used [1-4]. Considering that some limitations are indeed due to the use of parallel mechanisms, it is appealing to investigate architectures based on hybrid arrangements where serial and parallel concepts are combined [4]. The Tricept robot or Tricept machine tool is based on parallel tripod combined with passive chain, and equipped with serial 3- or 2- DOF wrist. The inventor of this structure is K.-E. Neuman [5], while the mechanics has been constructed by Neos [6].

The primary application of commercially available Tricept robots was the area of assembly where large insertion forces are required, e.g. as in the automobile industry. Other applications included deburring, milling, wood machining, laser and water-jet cutting, spot and laser welding.

The conceptual model of the Tricept based vertical five-axis machine tool considered in this paper, Figure 1a, is the basic option of the planned reconfigurable multi-axis machining system for HSC-milling of aluminium, steel as well as large size model making, plastic and foam machining.

The machine has a three-DOF structure of parallel type to execute translational motions and 2-DOF serial wrist to execute rotational motion i.e. tool orientation.

The basic module of Tricept based five-axis machine tool can be built as a plug-and-play module to configure different machines by placing it vertically Figure 1a, on

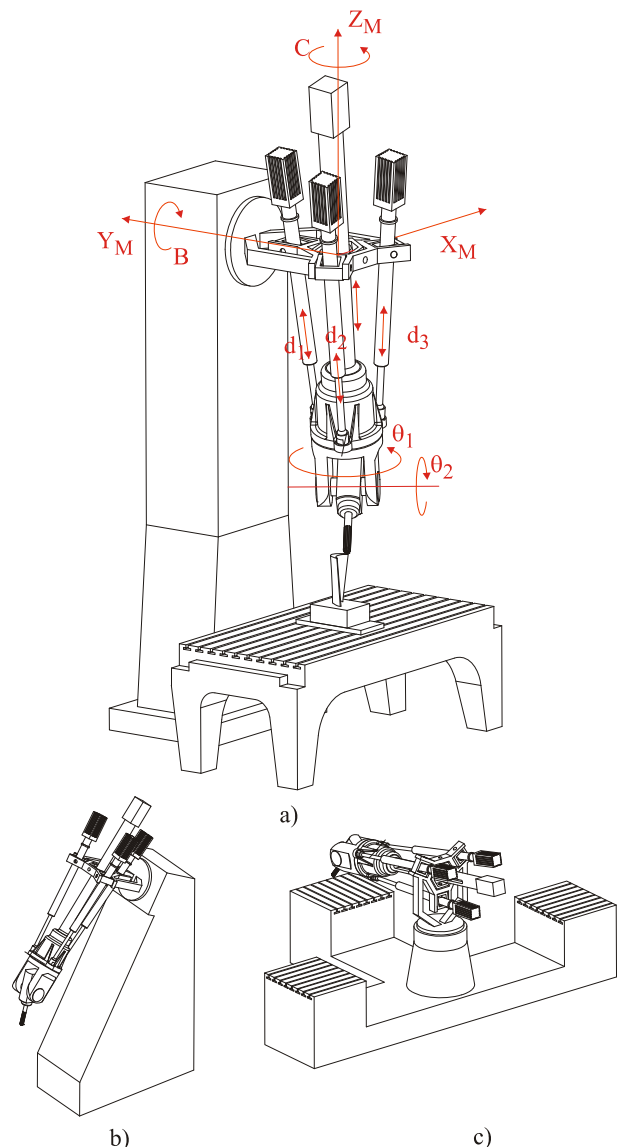an incline, Figure 1b, and horizontally, Figure 1c.

a)

b)   c)

Figure 1. Reconfigurability of the Tricept based machine tool

This paper is aimed at presenting a study on the kinematic modelling of the Tricept based five-axis machine tool. Since the machine comprises 3-DOF parallel structure and 2-DOF serial wrist direct and inverse kinematics also comprise serial and parallel part. Inverse kinematics is solved analytically while direct kinematics consists of an analytical and numerical part.

2. KINEMATIC MODELLING

Figure 2 represents a geometric model of the Tricept based vertical five-axis machine tool, Figure 1a, which comprises 3-DOF parallel structure and 2-DOF serial wrist. Parallel structure consists of four kinematic chains, including three variable length legs with identical topology and one passive leg connecting the fixed base B and the moving platform P. Three variable

length legs with actuated prismatic joints d_i, i =1,2,3 are connected to the base B by Cardan joints and to movable platform P by spherical joints. The fourth chain (central leg) connecting the centre of the base B to the platform P is passive constraining leg. It consists of a Cardan joint, a moving link, a prismatic joint and the second moving link fixed to the platform P. This fourth leg is used to constrain the motion of the platform to only 3-DOF. These 3-DOF are described by spherical coordinates i.e. by the axial translation $p_{Op} = \left| {}^M\mathbf{p}_{Op} \right|$

along the central leg and by two rotations Ψ and θ about two axes orthogonal to the central leg itself. Two-DOF serial wrist executes rotational motions i.e. tool orientation with actuated rotational joints θ_1 and θ_2.
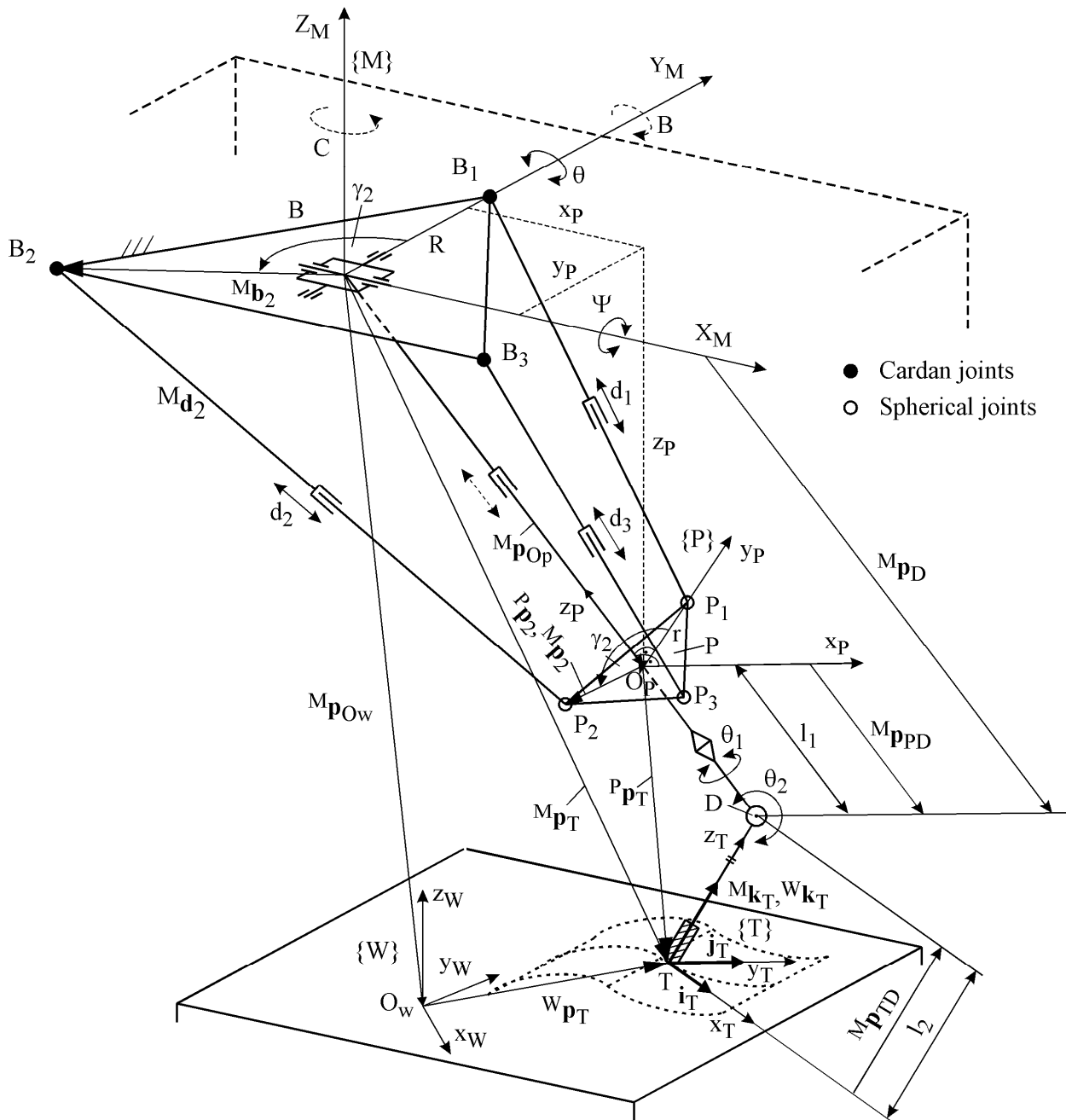

Figure 2. Geometric model of the Tricept based vertical five-axis machine tool

To adequately control the position and orientation of the tool during machining processes, kinematic model is required to establish mathematical description for the machine tool. Kinematic modelling of parallel structure involves solving inverse kinematics, Jacobian matrix as the basis for numerical solution of direct kinematics, and direct kinematics. Kinematic modelling for 2-DOF serial wrist involves solving direct and inverse kinematics in a well-known way [7-9]. Based on machine inverse kinematics the workspace has been analysed in order to select machine prototype design parameters.

2.1 Machine joint and world coordinates

As can be concluded from Figure 1a i.e. Figure 2, Tricept based five-axis machine tool will be considered below as a specific configuration of the five-axis vertical milling machine (X, Y, Z, B, C) spindle-tilting type [10].

The machine reference frame {M} has been adopted according to the standard for this machine type [11]. Frame {P} is attached to the moving platform in a way that z_p axis coincides with the axis of the central leg and with the axis of joint Θ_1. The tool frame {T} is attached to the milling tool at the tool tip T so that the axis z_t coincides with tool axis, and the frame {W} is attached to the work piece. Vectors $\mathbf{v}$ referenced in frames {M}, {W}, {P} and {T} are denoted by $M\mathbf{v}$, $W\mathbf{v}$, $P\mathbf{v}$ and $T\mathbf{v}$.

To solve direct and inverse kinematics, joint and world coordinates will be defined first.

Joint coordinates vector for this 5-axis Tricept based machine tool is represented as

$$\mathbf{q} = \begin{bmatrix} d_1 & d_2 & d_3 & \theta_1 & \theta_2 \end{bmatrix}^T \quad (1)$$

where d_i, $i=1,2,3$ and θ_i, $i=1,2$ are scalar joint variables controlled by actuators.

The description of world coordinates is based on tool path calculated by CAD/CAM systems defined by the set of successive tool positions and orientations in the work piece frame {W}, Figure 2. The thus calculated tool path is machine independent and is known as a cutter location file (CLF). A tool pose is defined by the position vector of the tool tip T in the work piece frame {W} as

$$^W\mathbf{p}_T = \begin{bmatrix} x_{Tw} & y_{Tw} & z_{Tw} \end{bmatrix}^T \quad (2)$$

and tool orientation is defined by unit vector of the tool axis as

$$^W\mathbf{k}_T = \begin{bmatrix} k_{Twx} & k_{Twy} & k_{Twz} \end{bmatrix}^T \quad (3)$$

As the axes of frames {M} and {W} need not be parallel, the tool tip position vector and unit vector of tool axis direction in the machine reference frame {M} can be expressed as

$$^M\mathbf{p}_T = \begin{bmatrix} X_M & Y_M & Z_M \end{bmatrix}^T = {}^M\mathbf{p}_{Ow} + {}^M_W R \cdot {}^W\mathbf{p}_T \quad (4)$$

$$^M\mathbf{k}_T = \begin{bmatrix} k_{Tx} & k_{Ty} & k_{Tz} \end{bmatrix}^T = {}^M_W R \cdot {}^W\mathbf{k}_T \quad (5)$$

where $^M\mathbf{p}_{Ow} = \begin{bmatrix} x_{Ow} & y_{Ow} & z_{Ow} \end{bmatrix}^T$ is the position vector of the origin of work piece frame {W}. It should be noted that determining the position vector $^M\mathbf{p}_{Ow}$ and orientation of the work piece frame {W}, is conducted according to the procedure for 5-axis CNC machine tools and thereafter the orientation matrix $^M_W R$ in equations (4) and (5) is determined and executed in a control system [9].

To complete the vector of world coordinates, it is also needed to determine the tool orientation angles B and C which define only the direction of tool axis z_T that also coincides with the axis of the last link i.e. motor spindle, Figure 2. Given that machine has 5 DOF, only the direction of the z_T axis is controllable, while the axes x_T and y_T will have uncontrollable rotation about the axis z_T.

The description of the position and orientation of one frame relative to another e.g. in this case of the frame {T} relative to the frame {M} can be represented through homogenous coordinate transformation matrix 4 x 4, [7,12,13], as

$$^M_T T = \left[\begin{array}{ccc:c} & ^M_T R & & ^M\mathbf{p}_T \\ \hdashline 0 & 0 & 0 & 1 \end{array} \right] =$$
$$= \left[\begin{array}{ccc:c} i_{Tx} & j_{Tx} & k_{Tx} & X_M \\ i_{Ty} & j_{Ty} & k_{Ty} & Y_M \\ i_{Tz} & j_{Tz} & k_{Tz} & Z_M \\ \hdashline 0 & 0 & 0 & 1 \end{array} \right] \quad (6)$$

where rotation matrix $^M_T R$ presents the orientation, while vector $^M\mathbf{p}_T$ presents the position of the frame {T} with respect to the machine reference frame {M}. To bring the tool axis i.e. the axis z_T of the frame {T} to a desirable angular position with respect to the frame {M}, the frame {T} must be rotated first about the axis Y_M by the angle B, and then about the axis Z_M by the angle C, as prescribed by the convention for 5-axis machine tools (X, Y, Z, B, C) spindle-tilting type. The derivation of equivalent rotation matrix $^M_T R$ can be further derived as

$$^M_T R = R_{ZM,C} \cdot R_{YM,B} =$$
$$= \begin{bmatrix} cC \cdot cB & -sC & cC \cdot sB \\ sC \cdot cB & cC & sC \cdot sB \\ -sB & 0 & cB \end{bmatrix} = \begin{bmatrix} i_{Tx} & j_{Tx} & k_{Tx} \\ i_{Ty} & j_{Ty} & k_{Ty} \\ i_{Tz} & j_{Tz} & k_{Tz} \end{bmatrix} \quad (7)$$

where rotation matrices $R_{YM,B}$ and $R_{ZM,C}$ are so called basic rotation matrices [13]. "c" and "s" refer to cosine and sine functions. As it is of interest only orientation of the tool axis z_T specified by unit vector $^M\mathbf{k}_T = \begin{bmatrix} k_{Tx} & k_{Ty} & k_{Tz} \end{bmatrix}^T$, whose description is above given by equating the corresponding members of matrix $^M_T R$ from equation (7) the angles B and C can be determined as

$$B = A\tan 2(\sqrt{1-k_{Tz}^2}, k_{Tz}) \qquad (8)$$

and

$$C = A\tan 2(k_{Ty}, k_{Tx}) \qquad (9)$$

Although in equation (8) a second solution exists, by using the positive square root the single solution for which $B \geq 0°$ is always computed [7,14]. As can be seen from equation (7), equation (9) is valid only when $sB \neq 0$ i.e. $B \neq 0°$. As tool can freely rotate in case when $B = 0°$ value for angle C can be arbitrary adopted. This way, the world coordinates vector of the machine can be expressed as

$$\mathbf{x} = \begin{bmatrix} X_M & Y_M & Z_M & B & C \end{bmatrix}^T \qquad (10)$$

2.2 Kinematic modelling of parallel mechanism

For further analysis it is necessary to specify world coordinates of the parallel mechanism first. As it was mentioned, the passive central leg is used to constrain the motion of the platform to only 3-DOF. According to Figure 2 these 3-DOF can be described by spherical coordinates

$$\mathbf{x}_{sp} = \begin{bmatrix} p_{Op} & \Psi & \theta \end{bmatrix}^T \qquad (11)$$

where:

- $p_{Op} = \left| {}^M\mathbf{p}_{Op} \right|$ is axial translation along central leg, and

- Ψ and θ are the rotation angles of the central leg's Cardan joint about axes X_M and Y_M respectively.

Vector ${}^M\mathbf{p}_{Op} = \begin{bmatrix} x_p & y_p & z_p \end{bmatrix}^T = \mathbf{x}_P$ is the position vector of origin Op of the frame {P} attached to the moving platform with respect to machine reference frame {M}, and represents Cartesian world coordinates vector.

As noticeable from Figure 2 joint axes of 2-DOF serial wrist intersect at point D (wrist centre). From this fact it is easy to conclude that the position of wrist centre D, i.e., ${}^M\mathbf{p}_D$ is influenced only by joint coordinates d_1, d_2, and d_3 of parallel mechanism.

For specified position vector of the tool tip ${}^M\mathbf{p}_T = \begin{bmatrix} X_M & Y_M & Z_M \end{bmatrix}^T$ and for specified tool orientation angles B and C the rotation matrix ${}^M_T R$ from equation (7) is calculated first. Then by using only vector ${}^M\mathbf{k}_T$ from calculated rotation matrix ${}^M_T R$ the position vector ${}^M\mathbf{p}_D$ of the wrist center D and its module p_D, according to Figure 2 can be calculated as

$$
{}^M\mathbf{p}_D = \begin{bmatrix} x_D \\ y_D \\ z_D \end{bmatrix} = {}^M\mathbf{p}_T + {}^M\mathbf{p}_{TD} =
$$

$$
= {}^M\mathbf{p}_T + l_2 \cdot {}^M\mathbf{k}_T = \begin{bmatrix} X_M + l_2 \cdot cC \cdot sB \\ Y_M + l_2 \cdot sC \cdot sB \\ Z_M + l_2 \cdot cB \end{bmatrix} \qquad (12)
$$

and

$$p_D = \left| {}^M\mathbf{p}_D \right| = \sqrt{x_D^2 + y_D^2 + z_D^2} \qquad (13)$$

As the position vectors ${}^M\mathbf{p}_{Op}$, ${}^M\mathbf{p}_D$ and ${}^M\mathbf{p}_{PD}$ are collinear and coincide with central leg, and as $\left| {}^M\mathbf{p}_{PD} \right| = l_1$ the module $p_{Op} = \left| {}^M\mathbf{p}_{Op} \right|$ can be calculated as

$$p_{Op} = p_D - l_1 \qquad (14)$$

Now, the description of the position and orientation of the frame {P} attached to the moving platform with respect to machine reference frame {M} can be represented as

$$
{}^M_P T = \begin{bmatrix} {}^M_P R & \vdots & {}^M\mathbf{p}_{Op} \\ \hline 0\ 0\ 0 & \vdots & 1 \end{bmatrix} \qquad (15)
$$

where rotation matrix ${}^M_P R$ represents the orientation while vector ${}^M\mathbf{p}_{Op}$ represents the position of frame {P} with respect to the machine frame {M}. Frame ${}^M_P T$ can be further derived using homogenous transformation matrices 4x4 as

$$
{}^M_P T = Trot_{(X_M, \Psi)} \cdot Trot_{(Y_M, \theta)} \cdot Ttran_{(Z_M, -p_{Op})} =
$$

$$
= \begin{bmatrix} c\theta & 0 & s\theta & \vdots & -p_{Op} \cdot s\theta \\ s\Psi \cdot s\theta & c\Psi & -s\Psi \cdot c\theta & \vdots & p_{Op} \cdot s\Psi \cdot c\theta \\ -c\Psi \cdot s\theta & s\Psi & c\Psi \cdot c\theta & \vdots & -p_{Op} \cdot c\Psi \cdot c\theta \\ \hline 0 & 0 & 0 & \vdots & 1 \end{bmatrix} = (16)
$$

$$
= \begin{bmatrix} {}^M_P R(\Psi, \theta) & \vdots & {}^M\mathbf{p}_{Op}(\Psi, \theta) \\ \hline 0\ 0\ 0 & \vdots & 1 \end{bmatrix}
$$

where

$$
{}^M\mathbf{p}_{Op} = \begin{bmatrix} -p_{Op} \cdot s\theta \\ p_{Op} \cdot s\Psi \cdot c\theta \\ -p_{Op} \cdot c\Psi \cdot c\theta \end{bmatrix} = \begin{bmatrix} x_p \\ y_p \\ z_p \end{bmatrix} \qquad (17)
$$

As the vectors ${}^M\mathbf{p}_D$ and ${}^M\mathbf{p}_{Op}$ are collinear, calculated components of vector ${}^M\mathbf{p}_D = \begin{bmatrix} x_D & y_D & z_D \end{bmatrix}^T$ in equation (12) can also be described by spherical coordinates according to equation (17) as

$$M\mathbf{p}_D = \begin{bmatrix} -p_D \cdot s\theta \\ p_D \cdot s\Psi \cdot c\theta \\ -p_D \cdot c\Psi \cdot c\theta \end{bmatrix} = \begin{bmatrix} x_D \\ y_D \\ z_D \end{bmatrix} \qquad (18)$$

From equations (18), (12) and (13) the platform's orientation angles Ψ and θ can be determined as

$$\theta = A\tan 2(x_D / - p_D, \sqrt{1 - (x_D / - p_D)^2}) \qquad (19)$$

$$\Psi = A\tan 2(y_D, -z_D) \qquad (20)$$

As can be seen from equation (18), equation (20) is valid when $c\theta \neq 0$ i.e. $\theta \neq \pm 90°$. This condition is always satisfied since angles Ψ and θ usually vary within the limits

$$-\frac{\pi}{3} \leq \Psi \leq \frac{\pi}{3} \text{ and } -\frac{\pi}{3} \leq \theta \leq \frac{\pi}{3} \qquad (21)$$

specified by the ranges of passive joints motions.

This way, the spherical world coordinates vector of parallel mechanism $\mathbf{x}_{sp}$ in equation (11) or Cartesian world coordinates vector $\mathbf{x}_p$ in equation (17) are completed.

2.3 Inverse kinematics of parallel mechanism

The inverse kinematics of parallel mechanism from Figure 2 deals with calculating the leg lengths d_i, i=1,2,3 when the platform pose is given.

Observing geometric relations in the example of a leg vector $^M\mathbf{d}_2$ shown in Figure 2, the following equations can be derived

$$^M\mathbf{d}_i = \begin{bmatrix} d_{ix} \\ d_{iy} \\ d_{iz} \end{bmatrix} = {}^M\mathbf{p}_{Op} + {}^M\mathbf{p}_i - {}^M\mathbf{b}_i =$$
$$= {}^M\mathbf{p}_{OP} + {}^M_P R(\Psi, \theta){}^P\mathbf{p}_i - {}^M\mathbf{b}_i, \ i = 1,2,3 \qquad (22)$$

where:

- $^M\mathbf{d}_i = \begin{bmatrix} d_{ix} & d_{iy} & d_{iz} \end{bmatrix}^T$, i=1,2,3 $\qquad (23)$

  are vectors of the actuated legs defined in the machine frame {M},

- $^M\mathbf{p}_{Op} = \begin{bmatrix} x_p & y_p & z_p \end{bmatrix}^T$ is the position vector of the origin Op of the frame {P} attached to the moving platform with respect to machine frame {M} and is given in equation (17),

- $^P\mathbf{p}_i = \begin{bmatrix} p_{ix} \\ p_{iy} \\ 0 \end{bmatrix} = \begin{bmatrix} r \cdot c\gamma_i \\ r \cdot s\gamma_i \\ 0 \end{bmatrix}$, i=1,2,3 are position

  vectors of the joint centres at the platform located on the circle of radius r with angular

position $\gamma_i = \frac{2\pi}{3}(i-1)$, and are defined in the frame {P},

- $^M\mathbf{p}_i = {}^M_P R(\psi, \theta) \cdot {}^P\mathbf{p}_i$, i=1,2,3 $\qquad (24)$

  are position vectors of the joint centres of the platform expressed in the machine frame {M},

- $^M\mathbf{b}_i = \begin{bmatrix} b_{ix} \\ b_{iy} \\ 0 \end{bmatrix} = \begin{bmatrix} R \cdot c\gamma_i \\ R \cdot s\gamma_i \\ 0 \end{bmatrix}$, i=1,2,3 are

  position vectors of the join centres at the base located on the circle of radius R with angular position $\gamma_i = \frac{2\pi}{3}(i-1)$ and are defined in the frame {M}.

By substituting corresponding vectors in equation (22) vectors $^M\mathbf{d}_i = \begin{bmatrix} d_{ix} & d_{iy} & d_{iz} \end{bmatrix}^T$, i=1,2,3 can be obtained from which inverse kinematics equations

$$d_i = = \sqrt{d_{ix}^2 + d_{iy}^2 + d_{iz}^2} \ , i=1,2,3 \qquad (25)$$

are derived as

$$d_1 = (p_{Op}^2 + r^2 + R^2 - 2 \cdot p_{Op} \cdot R \cdot c\theta \cdot s\Psi - \\ - 2 \cdot R \cdot r \cdot c\psi)^{1/2} \qquad (26)$$

$$d_2 = [p_{Op}^2 + r^2 + R^2 + p_{Op} \cdot R \cdot (c\theta \cdot s\Psi - \sqrt{3} \cdot s\theta) + \\ + \frac{r \cdot R}{2}(-3 \cdot c\theta - \sqrt{3} \cdot s\theta \cdot s\Psi - c\Psi)]^{1/2} \qquad (27)$$

$$d_3 = [p_{Op}^2 + r^2 + R^2 + p_{Op} \cdot R \cdot (c\theta \cdot s\Psi + \sqrt{3} \cdot s\theta) + \\ + \frac{r \cdot R}{2}(-3 \cdot c\theta + \sqrt{3} \cdot s\theta \cdot s\Psi - c\Psi)]^{1/2} \qquad (28)$$

This way, the joint coordinates vector of parallel mechanism can be expressed as

$$\mathbf{d} = \begin{bmatrix} d_1 & d_2 & d_3 \end{bmatrix}^T \qquad (29)$$

2.4 Jacobian matrix and direct kinematics of parallel mechanism

The direct kinematics problem for parallel mechanism consists of finding the vector of world coordinates $\mathbf{x}_{sp} = \begin{bmatrix} p_{Op} & \Psi & \theta \end{bmatrix}^T$ or $\mathbf{x}_P = \begin{bmatrix} x_p & y_p & z_p \end{bmatrix}^T$ as a function of joint coordinates $\mathbf{d} = \begin{bmatrix} d_1 & d_2 & d_3 \end{bmatrix}^T$. Generally, such problem does not have analytical solutions and different numerical algorithms based on Jacobian matrix are used.

Differential equations (26) – (28) with respect to the time the Jacobian matrix is obtained as

$$J = \begin{bmatrix} \dfrac{\partial d_1}{\partial p_{Op}} & \dfrac{\partial d_1}{\partial \Psi} & \dfrac{\partial d_1}{\partial \theta} \\ \dfrac{\partial d_2}{\partial p_{Op}} & \dfrac{\partial d_2}{\partial \Psi} & \dfrac{\partial d_2}{\partial \theta} \\ \dfrac{\partial d_3}{\partial p_{Op}} & \dfrac{\partial d_3}{\partial \Psi} & \dfrac{\partial d_3}{\partial \theta} \end{bmatrix} = \begin{bmatrix} J_{11} & J_{12} & J_{13} \\ J_{21} & J_{22} & J_{23} \\ J_{31} & J_{32} & J_{33} \end{bmatrix} \quad (30)$$

where:

$$J_{11} = (p_{Op} - R \cdot c\theta \cdot s\Psi)/d_1$$

$$J_{21} = [2 \cdot p_{Op} + R \cdot (c\theta \cdot s\Psi - \sqrt{3} \cdot s\theta)]/2 \cdot d_2$$

$$J_{31} = [2 \cdot p_{Op} + R \cdot (c\theta \cdot s\Psi + \sqrt{3} \cdot s\theta)]/2 \cdot d_3$$

$$J_{12} = (-p_{Op} \cdot R \cdot c\theta \cdot c\Psi + r \cdot R \cdot s\Psi)/d_1$$

$$J_{22} = [p_{Op} \cdot R \cdot c\theta \cdot c\Psi + r \cdot R \cdot (s\Psi - \sqrt{3} \cdot s\theta \cdot c\Psi)/2]/2 \cdot d_2$$

$$J_{32} = [p_{Op} \cdot R \cdot c\theta \cdot c\Psi + r \cdot R \cdot (s\Psi + \sqrt{3} \cdot s\theta \cdot c\Psi)/2]/2 \cdot d_3$$

$$J_{13} = p_{Op} \cdot R \cdot s\theta \cdot s\Psi / d_1$$

$$J_{23} = [p_{Op} \cdot R \cdot (-s\theta \cdot s\Psi - \sqrt{3} \cdot c\theta) +$$
$$+ r \cdot R \cdot (3 \cdot s\theta - \sqrt{3} \cdot c\theta \cdot s\Psi)/2]/2 \cdot d_2$$

$$J_{33} = [p_{Op} \cdot R \cdot (-s\theta \cdot s\Psi + \sqrt{3} \cdot c\theta) +$$
$$+ r \cdot R \cdot (3 \cdot s\theta + \sqrt{3} \cdot c\theta \cdot s\Psi)/2]/2 \cdot d_3$$

This so called analytical Jacobian matrix [15,16] relates the spherical velocity vector $\dot{\mathbf{x}}_{sp} = \begin{bmatrix} \dot{p}_{Op} & \dot{\Psi} & \dot{\theta} \end{bmatrix}^T$ to the joint velocity vector $\dot{\mathbf{d}} = \begin{bmatrix} \dot{d}_1 & \dot{d}_2 & \dot{d}_3 \end{bmatrix}^T$ and is used in this paper as a basis for simple numerical algorithm to solve direct kinematics for the purpose of simulation. For some advanced algorithms [16] so called geometric Jacobian matrix [15] that relates the Cartesian velocity vector $\dot{\mathbf{x}}_p = \begin{bmatrix} \dot{x}_P & \dot{y}_P & \dot{z}_P \end{bmatrix}^T$ to the joint velocity vector is used.

As it was mentioned, among several algorithms based on Jacobian matrix the simple numerical algorithm is selected to solve direct kinematics for the purpose of simulation. This algorithm is based on the constant Jacobian matrix calculated for the centre of workspace [17] i.e. for the initial position [18].

At step (n+1), the estimated position of the platform is given by

$$\mathbf{x}_{spn+1} = \mathbf{x}_{spn} + J^{-1}(\mathbf{x}_{sp0}, \mathbf{d}_0) \cdot (\mathbf{d} - \mathbf{d}_n) \quad (31)$$

where:

- $\mathbf{x}_{spn+1} = \begin{bmatrix} p_{Opn+1} & \Psi_{n+1} & \theta_{n+1} \end{bmatrix}^T$ is the estimated position of the platform at the step n+1,
- $\mathbf{x}_{spn} = \begin{bmatrix} p_{Opn} & \Psi_n & \theta_n \end{bmatrix}^T$ is the estimated position of the platform at the step n,
- $\mathbf{d}_n = \begin{bmatrix} d_{1n} & d_{2n} & d_{3n} \end{bmatrix}^T$ joint position (leg lengths) corresponding to the estimated platform position at the step n, result of the inverse kinematics of point $\mathbf{x}_{spn}$,
- $J^{-1}(\mathbf{x}_{sp0}, \mathbf{d}_0)$ is the inverse Jacobian matrix for the initial platform position $\mathbf{x}_{sp0}$ and joint position $\mathbf{d}_0$ as the result of inverse kinematics of point $\mathbf{x}_{sp0}$.

For the purpose of simulation, this algorithm converge in 1 to 5 steps, depending on the distance between the initial position and actual position. This comes from the large workspace of the parallel mechanism on one hand and the other hand from the high accuracy provided by predicted position sensors (this implies a high accuracy for the computation process). Consequently, the direct kinematics model takes almost twice as much time as the inverse model.

2.5 Kinematic modelling of 2-DOF serial wrist

To model 2-DOF serial wrist, the Denavit-Hartenberg (D-H) notation is used [7,19,20]. As noticeable from Figure 3 the serial wrist has two moving links connected together by two rotational joints. The first moving link is connected with supporting link fixed to moving platform {P} whose axis coincides with the axis of central leg. Second moving link is attached with a tool. To perform kinematic analysis, first coordinate frames are rigidly attached to each link. Relative position and orientation between these coordinate frames can be described by homogenous transformation traditionally referred to as an A matrix. Matrix $^{i-1}_i A$ [13] designates D-H transformation matrix relating frame (i) to frame (i-1). Figure 3 shows D-H coordinate frames for 2-DOF serial wrist in the reference position with respect to the platform frame {P}.
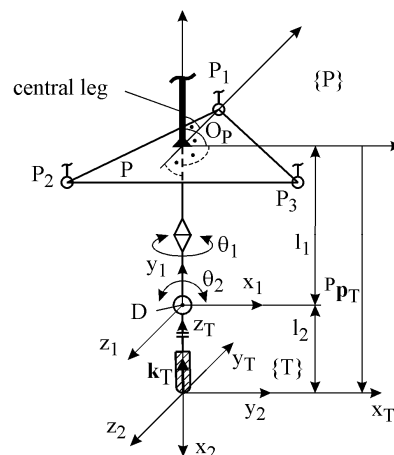

Figure. 3 Link coordinate frames for 2-DOF serial wrist in the reference position with respect to frame {P}

Prior to making the list of D-H parameters complete for each link of 2-DOF serial wrist, it is needed to make two important remarks:

- The frame {P} attached to the moving platform is adopted as the wrist reference frame;
- To make the wrist reference position second joint was rotated for $\theta_2 = -90°$ and tool frame {T} was introduced according to Figure 3.

Considering the above mentioned remarks a list of D-H parameters for each link is shown in Table 1.

Table 1. D-H kinematic parameters

Link i	$\alpha_i[°]$	$a_i[mm]$	$d_i[mm]$	$\theta_i[°]$
1	90	0	$-l_1$	θ_1
2	0	l_2	0	$\theta_2 - 90$

Substituting D-H parameters of the links from Table 1 the transformation matrices ^P_1A and ^1_2A are obtained first [13]. As noticeable from Figure 3, the tool frame {T} can be described relative to the frame (x_2, y_2, z_2) by homogenous transformation matrix as

$$
^2_T T = \begin{bmatrix} 0 & 0 & -1 & | & 0 \\ 1 & 0 & 0 & | & 0 \\ 0 & -1 & 0 & | & 0 \\ \hline 0 & 0 & 0 & | & 1 \end{bmatrix} \tag{32}
$$

Now, as it is well known [7,12,13], the tool position and orientation i.e. the position and orientation of frame {T} with respect to moving plate frame {P} (Figure 3) for the given joint coordinates θ_1 and θ_2 and specified link parameters can be determined as

$$
^P_T T = {}^P_1A \cdot {}^1_2A \cdot {}^2_T T = \left[\begin{array}{c|c} ^P_T R(\theta_1, \theta_2) & ^P\mathbf{p}_T(\theta_1, \theta_2) \\ \hline 0 \; 0 \; 0 & 1 \end{array} \right] =
$$

$$
\begin{bmatrix} c\theta_1 \cdot c\theta_2 & -s\theta_1 & -c\theta_1 \cdot s\theta_2 & | & l_2 \cdot c\theta_1 \cdot s\theta_2 \\ s\theta_1 \cdot c\theta_2 & c\theta_1 & -s\theta_1 \cdot s\theta_2 & | & l_2 \cdot s\theta_1 \cdot s\theta_2 \\ s\theta_2 & 0 & c\theta_2 & | & -(l_2 \cdot c\theta_2 + l_1) \\ \hline 0 & 0 & 0 & | & 1 \end{bmatrix} \tag{33}
$$

where

$$
^P\mathbf{p}_T = \begin{bmatrix} x_{TP} \\ y_{TP} \\ z_{TP} \end{bmatrix} = \begin{bmatrix} l_2 \cdot c\theta_1 \cdot s\theta_2 \\ l_2 \cdot s\theta_1 \cdot s\theta_2 \\ -(l_2 \cdot c\theta_2 + l_1) \end{bmatrix} \tag{34}
$$

This way, direct kinematics problem for 2-DOF serial wrist is solved locally with respect to frame {P}. Since, 2-DOF serial wrist is attached to the moving platform its solution of direct and inverse kinematic will be considered further as a part of complete machine inverse and direct kinematic solutions.

2.6 Machine inverse and direct kinematics

Using the determined position and orientation of the platform frame {P} with respect to the machine frame {M}, $^M_P T$ equation (16), and determined position and

orientation of the tool frame {T} with respect to the platform frame {P}, $^P_T T$ equation (33), the tool tip position and orientation with respect to machine frame {M} can be determined as

$$
^M_T T = {}^M_P T \cdot {}^P_T T =
$$

$$
= \left[\begin{array}{c|c} ^M_P R(\psi,\theta)^P_T R(\theta_1,\theta_2) & ^M_P R(\psi,\theta)^P\mathbf{p}_T(\theta_1,\theta_2) + ^M\mathbf{p}_{Op}(p_{Op},\psi,\theta) \\ \hline 0 \; 0 \; 0 & 1 \end{array} \right]
$$

$$
= \left[\begin{array}{c|c} ^M_T R(B,C) & ^M\mathbf{p}_T(X_M,Y_M,Z_M) \\ \hline 0 \; 0 \; 0 & 1 \end{array} \right] \tag{35}
$$

from which machine inverse and direct kinematics are solved.

Machine inverse kinematics:

Machine inverse kinematics comprises already analytically solved parallel part described in section 2.3 and serial part which will be considered in detail.

Parallel part of inverse kinematics:

For specified tool orientation angles B and C, the rotation matrix $^M_T R$ from equation (7) is calculated first. Then, by using only vector $^M\mathbf{k}_T$ from calculated matrix $^M_T R$, the position vector of wrist centre D, i.e. $^M\mathbf{p}_D$ equation (12), its module p_D, equation (13), and the module $P_{Op} = \left| ^M\mathbf{p}_{Op} \right|$, equation (14) are calculated. Using equations (18), (19) and (20) angles Ψ and θ are obtained.

By substituting calculated spherical coordinates p_{Op}, Ψ and θ into inverse kinematics (26) – (28) joint coordinates d_1, d_2 and d_3 are calculated i.e. parallel part of inverse kinematics is solved.

Serial part of inverse kinematics:

For inverse orientation kinematics i.e. calculation of joint coordinates θ_1 and θ_2 it is started from equation (35) from which only rotation matrices are used as

$$
^M_T R(B,C) = {}^M_P R(\psi,\theta) \cdot {}^P_T R(\theta_1,\theta_2) \tag{36}
$$

From equation (36) matrix $^M_T R(\theta_1,\theta_2)$ can be obtained as

$$
^P_T R(\theta_1,\theta_2) = {}^M_P R^{-1}(\psi,\theta) \cdot {}^M_T R(B,C) =
$$

$$
= {}^M_P R^T(\psi,\theta) \cdot {}^M_T R(B,C) \tag{37}
$$

Substituting matrices $^P_T R(\theta_1,\theta_2)$, equation (33), $^M_T R(B,C)$, equation (7) and $^M_P R(\psi,\theta)$, equation (16) into equation (37) it is obtained that

$$\begin{bmatrix} c\theta_1 \cdot c\theta_2 & -s\theta_1 & -c\theta_1 \cdot s\theta_2 \\ s\theta_1 \cdot c\theta_2 & c\theta_1 & -s\theta_1 \cdot s\theta_2 \\ s\theta_2 & 0 & c\theta_2 \end{bmatrix} =$$

$$= {}^M_P R^{-1}(\psi,\theta) \cdot {}^M_T R(B,C) = \begin{bmatrix} i_{TPx} & j_{TPx} & k_{TPx} \\ i_{TPy} & j_{TPy} & k_{TPy} \\ i_{TPz} & j_{TPz} & k_{TPz} \end{bmatrix} \quad (38)$$

As it is possible to control only the tool orientation axis z_T joint angles θ_1 and θ_2 can be determined by equating only corresponding members of the third columns of matrices from the left and right side in equation (38) as

$$\theta_2 = A\tan 2(\sqrt{1 - k_{TPz}^2}, k_{TPz}) \quad (39)$$

$$\theta_1 = A\tan 2(-k_{TPy}/s\theta_2, -k_{TPy}/s\theta_2) \quad (40)$$

where:

$$k_{TPz} = c\theta \cdot cC \cdot sB + s\psi \cdot s\theta \cdot sC \cdot sB - c\psi \cdot s\theta \cdot cB$$
$$k_{TPy} = c\psi \cdot sC \cdot sB + s\Psi \cdot cB \quad (41)$$
$$k_{TPz} = s\theta \cdot cC \cdot sB - s\psi \cdot c\theta \cdot sC \cdot sB + c\psi \cdot c\theta \cdot cB$$

As can be seen from equations (39), (40) and (41) the solutions for θ_1 and θ_2 depend on tool orientation angles B and C as well as on orientation angles Ψ and θ of the platform. Having calculated joint coordinates d_1, d_2 and d_3, equations (26) – (28), and θ_1 and θ_2, equations (39) – (41), solution of inverse kinematics problem of the machine is completed.

Machine direct kinematics:

Machine direct kinematics comprises parallel part already solved numerically in section 2.4 and a serial part which will be considered in detail.

Parallel part of direct kinematics:

For specified joint coordinates (leg lengths) $\mathbf{d} = \begin{bmatrix} d_1 & d_2 & d_3 \end{bmatrix}^T$ the initial position of the platform $\mathbf{x}_{SP0} = \begin{bmatrix} p_{Op} & \Psi_0 & \theta_0 \end{bmatrix}^T$ is adopted for which vector $\mathbf{d}_0 = \begin{bmatrix} d_{10} & d_{20} & d_{30} \end{bmatrix}^T$ is calculated using inverse kinematics (26) – (28). For adopted initial position $\mathbf{x}_{sp0}$ and calculated $\mathbf{d}_0$, constant Jacobian matrix $J(\mathbf{x}_{sp0}, \mathbf{d}_0)$ is calculated using equation (30) and then is inverted as $J^{-1}(\mathbf{x}_{sp0}, \mathbf{d}_0)$. Using numerical algorithm described by equation (31) the position vector of the platform expressed in spherical coordinates $\mathbf{x}_{sp} = \begin{bmatrix} p_{Op} & \Psi & \theta \end{bmatrix}^T$ is calculated. After calculating th coordinates p_{Op}, Ψ, and θ the frame ${}^M_P T$, i.e., rotation matrix ${}^M_P R$ and position vector ${}^M \mathbf{p}_{Op}$ from equation (16) are determined. This way direct kinematics of parallel part is completed.

Serial part of direct kinematics:

For determined spherical coordinates p_{Op}, Ψ, and θ in parallel part of direct kinematics, and for specified joint coordinates θ_1 and θ_2, matrix ${}^M_P R(\Psi,\theta)$, equation (16), vector ${}^M \mathbf{p}_{Op}(p_{Op}, \Psi, \theta) = \begin{bmatrix} x_P & y_P & z_P \end{bmatrix}^T$, equation (17), matrix ${}^P_T R(\theta_1, \theta_2)$, equation (33), and vector ${}^P \mathbf{p}_T(\theta_1, \theta_2) = \begin{bmatrix} x_{TP} & y_{TP} & z_{TP} \end{bmatrix}^T$, equation (34), are calculated first. Substituting them in equation (35) the position vector of the tool tip can be determined as

$${}^M \mathbf{p}_T = \begin{bmatrix} X_M \\ Y_M \\ Z_M \end{bmatrix} =$$
$$= \begin{bmatrix} c\theta \cdot x_{TP} + s\theta \cdot z_{TP} + x_P \\ s\Psi \cdot s\theta \cdot x_{TP} + c\Psi \cdot y_{TP} - s\Psi \cdot c\theta \cdot z_{TP} + y_P \\ -c\Psi \cdot s\theta \cdot x_{TP} + s\Psi \cdot y_{TP} + c\Psi \cdot c\theta \cdot z_{TP} + z_P \end{bmatrix} \quad (42)$$

After multiplying matrices ${}^M_P R$ and ${}^P_T R$ in (35) vector ${}^M \mathbf{k}_T$ is determined as

$${}^M \mathbf{k}_T = \begin{bmatrix} k_{Tx} \\ k_{Ty} \\ k_{Tz} \end{bmatrix} =$$
$$= \begin{bmatrix} -c\theta \cdot c\theta_1 \cdot s\theta_2 + s\theta \cdot c\theta_2 \\ -s\Psi \cdot s\theta \cdot c\theta_1 \cdot s\theta_2 - c\Psi \cdot s\theta_1 \cdot s\theta_2 - s\Psi \cdot c\theta \cdot c\theta_2 \\ c\Psi \cdot s\theta \cdot c\theta_1 \cdot s\theta_2 - s\Psi \cdot s\theta_1 \cdot s\theta_2 + c\Psi \cdot c\theta \cdot c\theta_2 \end{bmatrix} \quad (43)$$

from which tool orientation angles B and C can be calculated using equations (8) and (9) and direct kinematics of the machine is completed.

3. WORKSPACE ANALYSIS

Besides the selection of appropriate kinematic topology the most important step in the parallel machine design is to select the right geometric dimensions [19,20].

Based on inverse kinematics, it is possible to determine the position and orientation workspace of the Tricept based five-axis milling machine. The applied approach proved to be very useful and is based on the definition of position and orientation workspace for parallel kinematic chains [21].

In the case of the Tricept based five axis machine tool considered in this paper, the position and orientation workspace are given by

$$W_S(X_M, Y_M, Z_M, B, C) = \{0,1\} \quad (44)$$

which represents a Boolean function whose value is equal to 1 if the tool pose-defined by the quintet (X_M, Y_M, Z_M, B, C) is reachable without exceeding the limited motion range of the joints. Starting from the selected point in the workspace volume, the estimation is made by specific step-by-step strategy that locates tool in a given pose in the workspace and that

determines whether the pose is reachable or not by taking into account a limited motion range of the joints [10]. Based on selected prototype design parameters: R = 350mm, r=100mm, l_1=300mm, l_2=150mm, d_{min}=934mm, d_{max}=1520mm the determined workspace for three-axis machining ($B = 0°, C = 0°$, i.e., spindle axis is perpendicular to the $X_M Y_M$ plane) is shown in Figure 4.
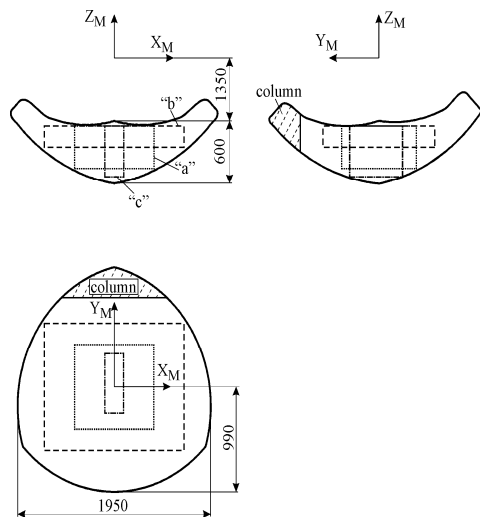

Figure 4. Workspace in the case of three-axis machining (B=0°, C=0°)

For programmers and operators familiar with CNC machine tools, the determined workspace can be reduced to the parallelepiped "a" as indicated in Figure 4. As it is known from practice, the adopted portion of workspace in the form of parallelepiped "a" can be changed in form "b" or "c" depending on the workpieces' shape and dimensions.

4. CONCLUSION

In order to develop reconfigurable multi-axis machining system for HSC-milling of aluminum, steel as well as large size model making a conceptual model of the Tricept based five-axis machine tool is discussed. The results of the study on the kinematic modelling of the vertical Tricept based five-axis machine tool have been in detail reported in this paper. For parallel structure, inverse kinematics is solved analytically while direct kinematics is solved numerically based on the constant Jacobian matrix calculated for the centre of workspace. Direct and inverse kinematics for 2-DOF serial wrist are solved analytically. Based on machine inverse kinematics, workspace has been analyzed in order to select machine prototype design parameters.

ACKNOWLEDGMENT

REFERENCES

[1] Weck, M and Staimer, D.: Parallel Kinematic Machine Tools - Current State and Future Potentials, Annals of the CIRP, Vol. 51, No. 2, pp. 671–681, 2002.

[2] Pritschow, G. and Wurst, K.H.: Systematic Design of Hexapods and other Parallel Link Systems, Annals of the CIRP, Vol. 46, No. 1, pp. 291–295, 1997.

[3] Warnecke, H.J., Neugebauer, R. and Wieland, F.: Development of Hexapod Based Machine Tool, Annals of the CIRP, Vol. 47, No. 1, pp. 337–340, 1998.

[4] Pierrot, F.: Towards non-hexapod mechanisms for high performance parallel machines, in: *Proceedings of 26th Annual Conference of the IEEE, IECON 2000*, Nagoya, Vol. 1, pp. 229 – 234.

[5] Neumann, K.-E.: Robot (US Patent 4,732,525, Neos Product HB, Norrtalije, Sweden, 1988).

[6] Neos Robotics, Home page at http://www.neorobotics.com/.

[7] Craig, J.J.: *Introduction to robotics: mechanics and control*, 2nd ed., Addison-Wesley, New York, 1989.

[8] Spong, M.W. and Vidyasagar, M: Robot Dynamics and Control, Wiley, Chichester, 1989.

[9] Milutinovic, D., Glavonjic, M., Slavkovic, N., Dimic, Z., Zivanovic, S., Kokotovic, B. and Tanovic, Lj.: Reconfigurable robotic machining system controlled and programmed in a machine tool manner, The international journal of advanced manufacturing technology, Vol. 53, No. 9-12, pp. 1217-1229, 2011.

[10] Milutinovic, M.: Diploma work (in Serbian), University of Belgrade, Mechanical Engineering Faculty, 2004.

[11] ISO 841:2001 Industrial automation systems and integration—Numerical control of machines—Coordinate system and motion nomenclature.

[12] Paul, R.P.: *Robot Manipulators: mathematics, programming and control*, MIT, Boston, 1981.

[13] Fu, K.S., Gonzalez, R.C. and Lee, C.S.G.: *Robotics: control, sensing, vision, and intelligence*, McGraw-Hill, New York, 1987.

[14] Lee, R.S. and She C.H.: Developing a postprocessor for three types of five-axis machine tools. Int J Adv Manuf Technol, Vol. 13, No. 9, pp. 658–665, 1997.

[15] Sciavicco, L. and Siciliano B.: *Modelling and Control of Robot Manipulators*, Springer, London, 2005.

[16] Siciliano, B.: The Tricept robot: Inverse kinematics, manipulability analysis and closed-loop direct kinematics algorithm, Robotica, Vol. 17, pp. 437-445, 1999.

[17] Merlet, J. P. and Pierrot, F.: Modeling of Parallel Robots, Modeling, in: Dombre, E., Khalil, W. (Ed.): Performance Analysis and Control of Robot Manipulators, ISTE USA, pp 81-134, 2007.

[18] Begon, Ph., Pierrot, F. and Dauchez, P.: High-precision, High-speed, Insertion with a 6 d-o-f parallel robot, in: *Proceeding of 24th International symposium on Industrial Robots*, 1993, Tokyo, pp. 145-152.

[19] Merlet, J.P.: *The Importance of Optimal Design for Parallel Structures*, in: Boer, C.R., Molinari-Tosatti, L., Smith, K.S. (Ed): *Parallel Kinematic Machines*, Springer Verlag, London, pp. 345-355, 1999.

[20] Milutinovic, D., Glavonjic, M., Kvrgic, V., and Zivanovic, S.: A New 3-DOF Spatial Parallel Mechanism for Milling Machines with Long X Travel, Annals of the CIRP, Vol. 54, No. 1, pp. 345–348, 2005.

[21] Innocenti, C. and Parenti, C.V.: Exhaustive enumeration of fully parallel kinematic chains, in: *Proceedings of the ASME Int. Winter Annual Meeting*, 1994, Chicago, USA, Vol. 55 pp. 1135–1141.

КИНЕМАТИЧКО МОДЕЛИРАЊЕ ХИБРИДНЕ ПАРАЛЕЛНО-СЕРИЈСКЕ ПЕТООСНЕ МАШИНЕ АЛАТКЕ

Милан Милутиновић, Никола Славковић, Драган Милутиновић

Паралелне структуре машина алатки и робота у односу на серијске структуре имају низ предности. За градњу паралелних машина алатки и робота данас се користи већи број механизама са паралелном кинематиком различитих топологија са 3 до 6 степени слободе. Међутим, с обзиром на извесна ограничења паралелних механизама интензивирана су истраживања на изналажењу механизама хибридних архитектура као комбинација паралелних и серијских структура. У раду су представљени резултати кинематичког моделирања хибридне паралелно-серијске петоосне машине алатке на бази Трицепт механизма. Како оваква машина укључује паралелну структуру са три степена слободе и серијску структуру са два степена слободе, то решења проблема инверзне и директне кинематике такође укључују паралелни и серијски део. Инверзни кинематички проблем је решен аналитички док решење директног кинематичког проблема садржи аналитички и нумерички део. На основу решења инверзног кинематичког проблема анализиран је радни простор у циљу избора пројектних параметара прототипа.